In-Situ Soft X-ray Absorption of Over-exchanged Fe/ZSM5

Willem M. Heijboer,[†] Andrea A. Battiston,[†,§] Axel Knop-Gericke,[‡] Michael Hävecker,[‡] Ralf Mayer,[‡] Hendrik Bluhm,[‡] Robert Schlögl,[‡] Bert M. Weckhuysen,[†] Diek C. Koningsberger,[†] and Frank M. F. de Groot*[,†]

Department of Inorganic Chemistry and Catalysis, Debye Institute, Utrecht University, Sorbonnelaan 16, 3584 CA Utrecht, The Netherlands, and Fritz-Haber-Institut der Max-Planck-Gesellschaft, Faradayweg 4-6, D-14195 Berlin, Germany

Received: January 16, 2003; In Final Form: August 27, 2003

In-situ soft X-ray absorption spectroscopy (XAS) has been applied to study the iron redox behavior in over-exchanged Fe/ZSM5. The Fe $L_{2,3}$ XAS and O K spectral shapes of the Fe/ZSM5 surface have been measured during heat treatments and reduction/oxidation cycles. Charge-transfer multiplet calculations provide a detailed understanding of the $L_{2,3}$ spectra of iron in Fe/ZSM5. The oxidized form of Fe/ZSM5 contains Fe^{III} ions in an octahedral surrounding, with a total crystal field splitting of ∼1.0 eV. This value is significantly smaller than that for Fe_2O_3, which is indicative of a much weaker Fe−O bonding. The reduced form of Fe/ZSM5 has Fe^{II} ions in a tetrahedral oxygen surrounding. The Fe $L_{2,3}$ spectra show that iron in calcined Fe/ZSM5 is reduced in 15 min to an average valence state of 2.65, under 10 mbar of pure helium at room temperature. This value has a relative uncertainty on the order of 0.01. Heating in helium up to 350 °C under the same pressure further reduces the iron valence to 2.15. The oxygen spectra show that the autoreduction is accompanied by a loss of molecular oxygen and water. Reoxidation with 5% O_2 in helium yields a valence of >2.90 after 10 min.

Introduction

Photons in the soft X-ray range (100−1000 eV) are suitable probes for the electronic structure of a reacting catalyst surface. Because of the use of the electron-yield detection mode, the X-ray absorption signal is surface sensitive. In-situ soft X-ray absorption spectroscopy (XAS) has been introduced by Knop-Gericke and co-workers.[1−3] For example, by measuring the Cu $L_{2,3}$-edge of the surface and the O K spectra for the surface and the gas phase, a new form of weakly bound oxygen was discovered that only exists under the reaction conditions and can be correlated with the selective oxidation reaction.

Fe/ZSM5 is a catalyst that can be used for a variety of reactions, depending on the iron loading, preparation method, thermal treatment, and activation procedure. For example, low-loaded, isomorphously substituted Fe/ZSM5, after steaming at 550 °C, is very active in the decomposition of N_2O to nitrogen and oxygen and the subsequent direct oxidation of benzene to phenol.[4,5] Over-exchanged Fe/ZSM5 with a high iron loading (up to 5 wt %) is an effective catalyst for the selective catalytic reduction of NO_x using hydrocarbons.[6,7] The amount of iron present in the catalyst can be tuned by the manner of preparation. In general, the substitution of iron in the framework of ZSM5 results in a maximum iron loading of 1 wt %. By introducing iron in extra framework positions (for example, via ion exchange or sublimation), a higher loading is possible. The sensitivity of iron species toward washing, calcination, steaming, reduction, and oxidation treatments is different for different locations within the zeolite. Battiston and co-workers[8] extensively investigated the structures of the different Fe species obtained after the different steps in the preparation procedure, using the sublimation of $FeCl_3$. In addition, a severe calcination procedure (heating rate of 5 °C/min), as used in the literature, leads to binuclear Fe centers to some larger iron oligomers inside the zeolite channels. In addition, one finds the formation of iron oxide clusters on the outside of the ZSM5 crystals. By applying a mild calcination (a heating rate of 0.5 °C/min) the amount of binuclear Fe species seems to account for ∼80% of the total iron amount. The binuclear Fe species are believed to be the catalytic active centers for the reduction of NO_x.[9] A precise characterization of the iron phases in Fe/ZSM5 is complicated, particularly without the use of in-situ studies. The presence of catalytic inactive Fe species (spectators) complicates the identification of the active Fe phase.

Garten and co-workers showed that the iron in zeolite Y exhibits autoreduction upon heating and evacuation.[10] Several other authors confirmed the autoreduction ability of iron in Fe/ZSM5[11−14] and, generally, the sensitivity toward the autoreduction of metal oxide complexes.[15,16] Battiston and co-workers[9] studied the autoreduction behavior of the Fe/ZSM5 catalyst that was prepared via the mild calcination route with Fe K-edge XAFS. The authors observed that the binuclear Fe species present could be reduced in helium at 350 °C to an average Fe valence of ∼2.4. In this paper, we applied in-situ soft XAS to further determine the structural and electronic properties of the Fe species present in Fe/ZSM5.

We will demonstrate that Fe $L_{2,3}$ XAS is a valuable technique that can be applied in-situ and allows for a precise determination of the valence of iron. We will study the oxidation and reduction behavior of the Fe sites in Fe/ZSM5 and determine the iron valence under various conditions. By simulating the experi-

* Author to whom correspondence should be addressed. E-mail: F.M.F.deGroot@chem.uu.nl.
† Debye Institute, Utrecht University.
‡ Fritz-Haber-Institut der Max-Planck-Gesellschaft.
§ Present address: Research Facility, Akzo Nobel Catalysts, 1030 BE, Amsterdam, The Netherlands.

10.1021/jp034125c CCC: $25.00
Published on Web 11/04/2003

TABLE 1: Fe/ZSM5 Samples Used in the Measurements

sample	measurement conditions	catalyst pretreatment
Fe/ZSM5-A	Fe/ZSM5 under 5% O_2 in helium (reoxidized)	calcination ramp of 5 °C/min
Fe/ZSM5-B	Fe/ZSM5 under 5% H_2 in helium (reduced)	calcination ramp of 5 °C/min
Fe/ZSM5-C	Fe/ZSM5 under 5% H_2 in helium (reduced)	calcination ramp of 0.5 °C/min

mental spectral shape, detailed information about the coordination of Fe can be obtained. We will measure the valence of iron in Fe/ZSM5 in a helium atmosphere at room temperature and during heating to 350 °C with a time resolution of ~1 min. In addition, the detection of the O K-edge of the gas phase will be used to check the development of the presence of water and molecular oxygen. In a subsequent paper, we will present a more extensive study on Fe/ZSM5 that has been prepared via mild calcination. This additional study will show that the application of in-situ soft X-ray spectroscopy can give relevant information about the catalytic active Fe sites.

2. Experimental Section

2.1. Catalyst Preparation and Characterization. Fe/ZSM5 was prepared via the $FeCl_3$ sublimation method proposed by Chen and Sachtler.[17] NH_4/ZSM5 (Si/Al = 17), obtained from Zeolyst, was converted to the H^+ form by calcination in O_2 at 550 °C for 3 h. The calcined H/ZSM5 (1.0 g) was flushed overnight in a helium flow (40 mL/min) at 300 °C. Then, 0.31 g of anhydrous $FeCl_3$ (98%, Acros Organics) was loaded and the sublimation exchange procedure was performed at 330 °C for 30 min. After sublimation, the sample was washed in 1000 mL of doubly deionized H_2O for 30 min, dried overnight in air at 70 °C, and calcined for 3 h in flowing O_2 at 350 °C.

The HCl formed during the $FeCl_3$ reaction with the Brønsted acid sites of the H/ZSM5 was absorbed in a NaOH solution, and acid−base titration of the remaining OH^- in the solution was used to quantify the amount of HCl released during the $FeCl_3$ exchange. The ratio between the HCl produced during the sublimation reaction and the H^+ sites that are theoretically present in the support, by assuming $Al/H^+ = 1$, was used to calculate the H^+ removal efficiency, according to the reaction $Fe_2Cl_6 + 2H^+ \rightarrow 2HCl + [Fe_2Cl_4]^{2+}$.

Details about the sample preparation were described earlier by Battiston et al.[18] Almost all Brønsted acid sites were removed from the H/ZSM5, considering that the H^+ removal efficiency value of 0.98. Inductively coupled plasma (ICP) analysis was performed to determine the Si/Al ratio (Si/Al = 17.0) and the iron loading (Fe/Al = 0.97) of the starting Fe/ZSM5 sample. This implies that the iron weight percentage is 4.71. The sample was heated under flowing oxygen at a rate of 120 mL/min in a tubular oven, using a temperature ramp of 5 °C/min, and calcined at 550 °C for 3 h. The crystalline fingerprint of the zeolite support was monitored after each synthesis step using XRD. On the basis of these measurements, lattice damage or significant formation of large iron oxide particles could be excluded. X-ray absorption experiments were conducted to investigate the valence of iron and the nature of the evolving gases during various chemical and heat treatments. The Fe/ZSM5 samples that are described in Table 1 will be used.

2.2. In-Situ Soft X-ray Absorption Spectroscopy. The soft X-ray absorption spectra of the Fe $L_{2,3}$-edge (700−730 eV) and the O K-edge (525−550 eV) were measured at BESSY (Berlin), using beamlines U49/2-PGM-1 and UE56/2-PGM-1. The spectral resolution of the monochromators was ~0.2 eV. The instrumentation for in-situ low-energy XAS experiments has been developed by Knop-Gericke and co-workers and is described in detail elsewhere.[1−3] We used a stainless-steel in-situ cell in which the powdered zeolite sample was fixed in a sample holder. The flow rates of helium and of 5% O_2/helium was 100 mL/min, of which approximately half entered the in-situ cell. A homemade gas-mixing system regulated the flow, and the total pressure was ~10 mbar during the experiments. The temperature was increased from room temperature to the reaction temperature of 350 °C, using a ramp rate of 5 °C/min.

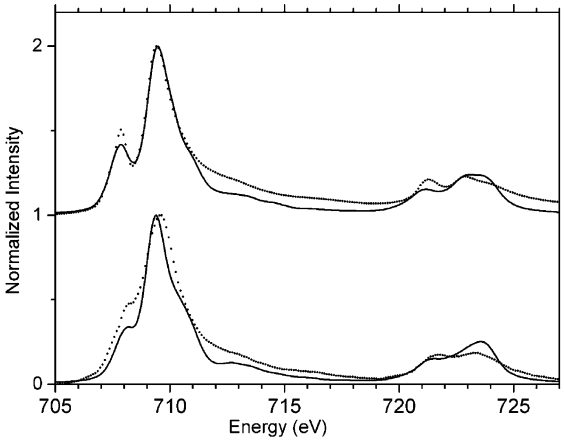

Figure 1. Charge-transfer multiplet (CTM) simulations (solid lines) compared with the experimental spectra (dotted lines) of Fe_2O_3 (top spectra) and Fe/ZSM5-A (bottom spectra).

The X-ray absorption spectral shape is measured with two collector plates that detect the ionized gas that is due to the created electrons in the X-ray absorption process and the subsequent nonradiative decay of the core hole, i.e., ionized-gas conversion total electron yield, with a probing depth of ~4 nm.[19] One detector measures the gas phase, while a second detector (close to the sample surface) detects both the gas phase and surface signal, where "surface" is defined here as the top 4 nm of the sample. The surface signal can be revealed through subtraction of the gas-phase signal. The energy scale was calibrated with the O peak position of O_2[20] and the Fe peak position of Fe_2O_3.[21] After background subtraction, all spectra were normalized to 1.0, because yield methods in X-ray absorption only scale with the absorption cross section but are not capable of measuring the absolute absorption cross sections.

3. Results

3.1. The Fe $L_{2,3}$ Spectra. The Fe 2p X-ray absorption spectral shape has peaks at ~712 eV for the L_3-edge and 725 eV for the L_2-edge, where the energy splitting is given by the 2p spin−orbit coupling. Figure 1 compares the Fe $L_{2,3}$ spectrum of Fe/ZSM5-A with that of Fe_2O_3. The Fe_2O_3 spectrum is identical to the spectra published in the literature.[21−24] These references also include the $L_{2,3}$ X-ray absorption spectra of FeO, Fe_3O_4, and other iron oxides. The spectra of both Fe/ZSM5-A and Fe_2O_3 have been analyzed with the charge-transfer multiplet (CTM) program.[25−28] The Fe $L_{2,3}$ spectrum of Fe_2O_3 is used as a reference and the spectrum shown is measured at the same beamline, to compare the experimental resolution. It corresponds well to the theoretical curve that has been calculated using a ground-state description of the Fe^{III} site given with two configurations, respectively $3d^5$ and $3d^6\underline{L}$. The $\underline{L}$ denotes a

TABLE 2: Charge-Transfer Parameters[a] as Used in the Simulations of the Fe $L_{2,3}$ Spectra

	10Dq(ion)	charge-transfer energy, Δ	$T(E_g)$	$T(T_{2g})$	symmetry	geometry
Fe_2O_3	1.1	3	2	1	$^6A_1$	octahedral
Fe/ZSM5-A	0.7	3	2	1	$^6A_1$	octahedral
Fe/ZSM5-C	−1.0	4	1	2	^5E	tetrahedral

[a] All numerical values given in electron volts (eV).

ligand hole, i.e., a hole on the O neighbors that surround the Fe atom under consideration. Within the CTM model, the ground state is defined by several parameters, as given in Table 2. The first two columns respectively show the ionic value of the cubic crystal field (10Dq(ion)) and the charge-transfer energy (Δ), which defines the energy difference between the $3d^5$ and $3d^6\underline{L}$ configurations. These configurations are split by multiplet effects and spin−orbit couplings, for which we use the atomic values.[27] The third and fourth columns contain the mixing terms for E_g and T_{2g} hopping, respectively. E_g hopping implies that an electron is moved from an oxygen orbital to a metal E_g orbital. In an octahedral crystal field, E_g hopping is approximately twice as strong as T_{2g} hopping, as is confirmed from the experiments and from density function calculations.[27] The fifth and sixth columns give the local geometry and site symmetry of the iron site, respectively. The spectral shape of Fe/ZSM5-A can be explained well from the same configurations, although with a reduced ionic crystal field splitting of 0.7 eV. The mixing of the $3d^5$ and $3d^6\underline{L}$ configurations adds an additional 0.3−0.4 eV to the overall splitting between the E_g and T_{2g} states. This implies that the overall crystal-field splitting is 1.4 eV for Fe_2O_3 and 1.0 eV for Fe/ZSM5-A. The reduced crystal-field splitting is particularly evident in the first peak, which is reduced in intensity and shifted closer to the main peak. The CTM analysis shows that Fe/ZSM5-A is indeed completely oxidized to a trivalent state, within an octahedral surrounding. It is noted that this Fe/ZSM5-A sample is reoxidized after first being reduced. The fact that the crystal-field splitting of Fe/ZSM5-A is considerably smaller than that for Fe_2O_3, which suggests (on average) less bonding between Fe and its six O neighbors. Depending on the particular model used, these six O neighbors may belong to the zeolite framework, hydroxyl groups, adsorbed water, and bridging O atoms.

Both Fe_2O_3 and Fe/ZSM5-A have a $^6A_1$ ground state that has all the spin-up electrons filled, ($t_{2g}^3e_g^2\{up\}$) and all the spin-down states empty. This special characteristic makes the spectrum rather insensitive to small geometric distortions. This implies that the geometric symmetry can be determined as octahedral-like, but small distortions will not be detectable.

Figure 2 shows the Fe/ZSM5-B and Fe/ZSM5-C spectra in comparison with an Fe^{II} simulation for tetrahedral symmetry. A CTM calculation has been used, with the parameters as given in Table 1. The ionic crystal-field splitting is −1.0 eV, where the negative sign implies that the energy ordering of the T_{2g} and E_g orbitals is reversed with, for a tetrahedral crystal field, the T_{2g} antibonding states at higher energy, because of their larger interaction with the neighboring O atoms. An ionic crystal field of −1.3 implies a total crystal-field splitting of approximately −1.3 eV. The ground state has ^5E symmetry, which implies that the sixth 3d electron occupies an e_g orbital. Figure 2 shows that a good agreement with the spectrum has been obtained. The top portion of the figure shows a comparison of the spectrum of Fe/ZSM5-B (dashed−dotted line) with that of Fe/ZSM5-C (dotted line). The bottom portion of the figure shows a comparison of the spectrum of the Fe/ZSM5-C sample (the dashed-dotted line) with the theoretical spectrum (solid line). The Fe/ZSM5-B sample is expected to contain some 20-nm-size Fe_2O_3 particles on the outside of the zeolite crystal, which prevents the sample from being completely reduced to the divalent state.[9] The Fe/ZSM5-C sample has been completely reduced, as is shown by the good agreement between the simulation and the experiment. The valence of Fe/ZSM5-B is simulated by adding the experimental spectra of Fe/ZSM5-A and Fe/ZSM5-C, yielding a value of 2.16. Disregarding the estimated maximum systematic error of 5%, this value has a relative uncertainty on the order of 0.01. This high accuracy is possible because the "reference spectra" of Fe/ZSM5-A and Fe/ZSM5-C are very closely related to the actual spectra of the Fe/ZSM5 system at various temperatures and gas conditions. This strong similarity allows for a smaller error bar, with respect to the general methods that have been derived, for example, by Van Aken and Liebscher.[21] In this paper, which involves iron oxide minerals, several detailed analysis procedures are compared, and it is found that, for a wide range of iron oxide minerals, good estimates could be made of the oxidation state from peak fitting (with an error of <0.04) and reference spectra fitting (with an error of <0.02). Given the similarity of the reference compounds, this allows for an uncertainty on the order of 0.01 for the Fe/ZSM5 systems.

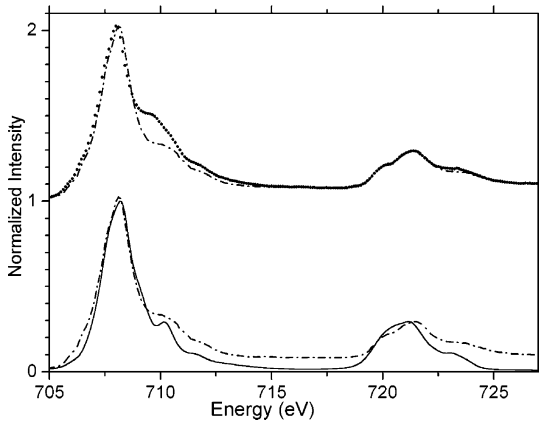

Figure 2. (Top) Experimental spectra of Fe/ZSM5-C (dashed−dotted line) and Fe/ZSM5-B (dotted line). (Bottom) CTM simulation (solid line) compared with the experimental spectrum of Fe/ZSM5-C (dashed−dotted line).

We conducted extensive searches for a possible octahedral ground-state situation; however, none of the reasonable descriptions of the ground state came close to describing the Fe 2p X-ray absorption spectral shape. In particular, the octahedral complexes do give a systematically larger value for the splitting between the L_3 and L_2 structures. This rules out an octahedral surrounding for Fe^{II} and implies that the sixth electron indeed occupies an e_g orbital. There can be, and most likely will be, symmetry distortions from a pure tetrahedral surrounding. If these symmetry distortions are small, their effect on the spectral shape also will be small. In addition, in the likely case that there will be a range of different distortions, the only expected effect is a broadening of the spectral shape. In conclusion, it can be stated that octahedral Fe^{III} sites in oxidized Fe/ZSM5 change to tetrahedral Fe^{II} sites in reduced Fe/ZSM5. Later in this paper, we will show that this is a reversible process.

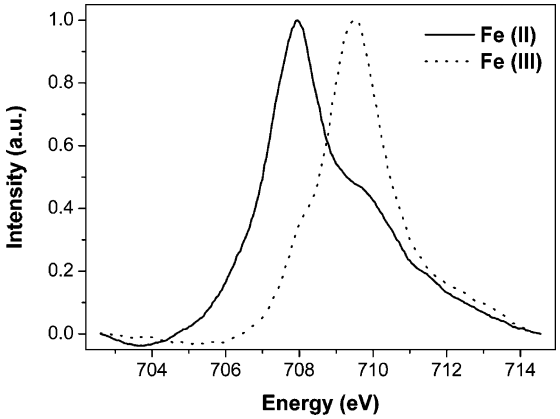

Figure 3. Fe L_3 X-ray absorption spectra of Fe/ZSM5-A (dotted line, Fe^{III}) and Fe/ZSM5-C (solid line, Fe^{II}) as used in the fast valence determination method.

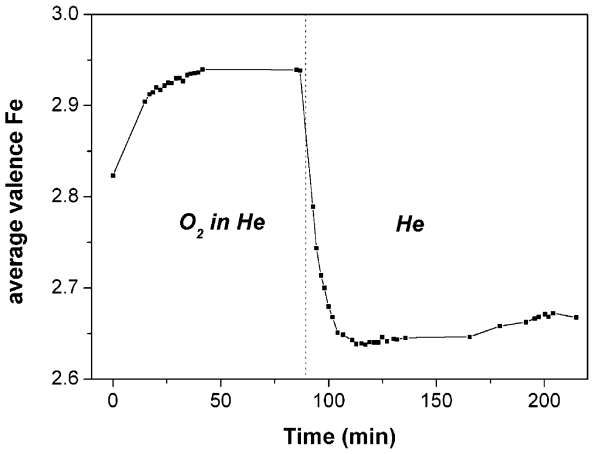

Figure 4. Oxidation in an O_2 atmosphere, followed by autoreduction in helium, of iron in Fe/ZSM5-A samples at room temperature.

3.2. Autoreduction in Helium. Each Fe $L_{2,3}$ spectrum can be considered as a linear combination of the reference spectra of Fe/ZSM5-A and Fe/ZSM5-C. To accelerate the measurement time to 50 s, we have not measured the entire $L_{2,3}$ spectrum, but rather only the L_3-edge. Figure 3 compares the two reference spectra for this energy range, i.e., the Fe L_3 spectra of Fe/ZSM5-A and Fe/ZSM5-C. In principle, each measured spectrum can be simulated from the addition of the Fe^{II} and Fe^{III} spectra. It has been checked in detail that this procedure can accurately be replaced by a procedure for which one measures the intensities at the peak positions for Fe^{II} (707.9 eV) and Fe^{III} (709.5 eV) and scales the intensity ratio to the theoretical curves. In other words, the ratio between the two peaks at the given energies can be considered as a measure for the average oxidation number. By analyzing the spectra as such, we were able to monitor the mean valence of the iron present in Fe/ZSM5 during treatments at temperatures in the range of 25−350 °C and with gas flows of helium and O_2. The relative uncertainty in the effective valence of iron, estimated from the addition of spectra, is ∼0.02. Fast Fe L_3 measurements with intervals of 50 s were taken in the energy range of 702.5−714.5 eV. Periodically, we recorded the complete Fe $L_{2,3}$ spectral shape to check potential variations in the background.

Figure 4 shows the variation of the average valence state under the oxidation, with 5% O_2 in helium, of calcined Fe/ZSM5 at room temperature and a pressure of 2 mbar. The oxidized form is subsequently exposed to helium for 2 h. The valence of the Fe/ZSM5-A sample under 5% O_2 in helium at room temperature first shows an oxidation to a valence of 2.94

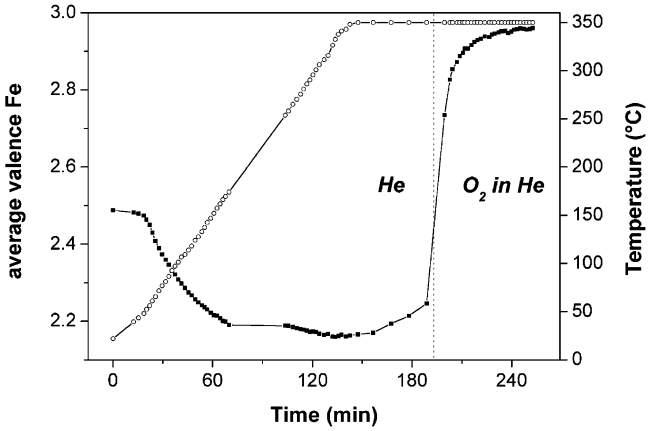

Figure 5. Progressed autoreduction, in helium, of iron in Fe/ZSM5; conditions were heating from 20 °C to 350 °C, followed by reoxidation in an O_2 atmosphere at 350 °C. Legend is as follows: (■) average valence of the Fe ion (left axis), (○) temperature (right axis).

± 0.01 and stays constant at this value for 50 min. At t = 90 min, we switch to pure helium, after which time the sample is reduced in 15 min to a minimum valence of 2.64, followed by a slight reoxidation to a value of ∼2.68 after 200 min. Figure 4 shows that, even at room temperature, the Fe/ZSM5 system is subject to significant autoreduction. A possible explanation of the reoxidation from 2.65 to 2.68 is a slight reoxidation that is due to O_2 that comes from the bulk. As previously mentioned, soft X-ray absorption measures only the top 4 nm of the sample, and the autoreduction can be expected to be faster at the surface than in the bulk. This observation indicates a very dynamic local valence that will be considered further in the discussion below. Next, we investigated the difference between the X-ray irradiated portion of the sample and a fresh spot. The valence of the spot that was irradiated for 200 min is 2.68, and a fresh spot had an average valence of 2.49. Apparently, an irradiated area has a higher mean valence. This is not obvious, because the temperature effect of the irradiation will tend to decrease the valence, as will be discussed below. Apparently, the temperature effect is not important and the ionizing effect of the X-ray tends to reoxidize the Fe sites. A re-reduction effect of irradiation on the valence state is observed for almost-trivalent iron at high temperatures. In that case, the change to a nonirradiated spot displays a lower valence state. It can be concluded that, upon irradiation, the average valence state of iron changes faster to its equilibrium state than a nonirradiated portion of the sample.

To investigate the stability of the iron phase that is present at the zeolite surface at the reaction temperature for the deNO_x reaction, 350 °C, we recorded Fe L_3 spectra while heating the Fe/ZSM5 from 25 °C to 350 °C, at a rate of 5 °C/min, at 2 mbar of helium. The result is shown in Figure 5. During heating from room temperature to 350 °C, the mean valence is reduced from 2.49 to 2.16. The starting valence is 2.49, because we used a nonirradiated starting position of the sample, as discussed previously. The gap between t = 70 min and t = 100 min is related to a re-injection of electrons into the storage ring. After reaching the final temperature of 350 °C, we again observe a slight reoxidation. As discussed previously, a likely explanation is the reoxidation of the surface Fe^{II} sites with O_2 that comes from the bulk (in other words, the equilibration between the valence at the surface and in the bulk). Reoxidation in 5% O_2 in helium at 350 °C yields an Fe valence of >2.90 after 10 min, demonstrating that the autoreduction of iron in Fe/ZSM5 is a fast, reversible process.

3.3. Oxygen K-Edge Spectra. The in-situ cell and detection setup allows for the simultaneous measurement of the sample

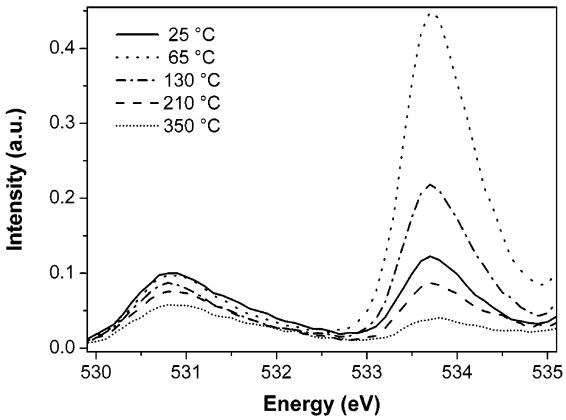

Figure 6. Evolution of the O K-edges during autoreduction in helium at selected temperatures in the range of 25−350 °C. (Not all measured temperatures are shown.)

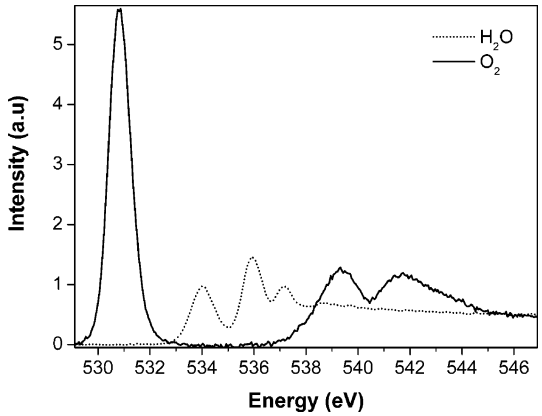

Figure 7. O 1s X-ray absorption for molecular oxygen (solid line) and water (dotted line). Gas-phase oxygen and water reference spectra have been replotted from the COREX database.[25]

and gas-phase signal. This is not important for the Fe L-edge, because there is no gas-phase iron. However, it opens the possibility to measure the gas-phase and surface signal of the O K-edge at 530 eV. We also measured, during the heat treatment in helium (shown in Figure 5), the O K-edge spectrum of the gas phase above the catalyst surface. In Figure 6, we show the results of the O K-edge spectra of the gas phase at different temperatures while flushing the cell with purified helium. Figure 7 shows that the first peak (530.8 eV) can be assigned to molecular oxygen (O_2).[29] The second peak in Figure 6 belongs to the three-peak feature of water. Figure 7 shows the full water spectrum with peaks at 533.7, 535.7, and 536.9 eV. For clarity, in Figure 6, only the first of the H_2O peaks is shown, where we have checked that the ratio between the three peaks is the same for all temperatures and spectra measured.

Figure 8 summarizes the results in a graph that represents the trends in O_2 and H_2O evolution during heating of Fe/ZSM5 in helium. The presence of the O_2 peak at room temperature indicates the release of O_2 from the zeolite already at this temperature. The peak decreases with the temperature. Comparison of this figure with the iron valence (Figures 4 and 5) shows that this formation of O_2 is proceeding simultaneously with the autoreduction process of iron. To probe the amount of oxygen and water formed qualitatively, we defined the intensity integral for O_2 for the photon-energy range of 530.0−532.9 eV and H_2O for 533.0−535.2 eV. Figure 8 shows that the autoreduction of iron in helium is accompanied by the release to the gas phase of O_2 and H_2O over the entire temperature range of 25−350 °C. The signal that is due to the water reaches

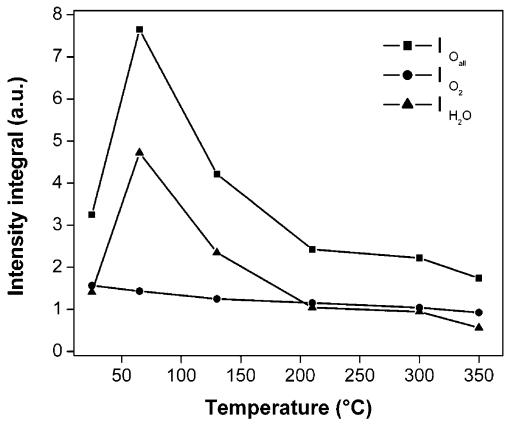

Figure 8. Trends in the O_2 and H_2O evolution during the heating of Fe/ZSM5 in helium.

a maximum intensity at a temperature of 75 °C and, at higher temperatures, declines in intensity. The release of O_2 slowly decreases from 25 °C to higher temperatures. It is noted that, in addition to the water produced during the iron autoreduction process, it is likely that another contribution for water release can be attributed to physisorbed water that comes from the surface and out of the channels of the zeolite upon heating.

4. Discussion

In the calcination procedure (using a temperature ramp of 5 °C/min), agglomeration of the binuclear Fe complexes toward inactive oxide/hydroxide clusters is significant.[8] Thus, some of the iron is present in the form of iron oxide clusters instead of binuclear clusters. The iron in the iron oxide clusters is octahedral Fe^{III} and also the binuclear complexes contain octahedral Fe^{III}. Figure 9a shows a possible structure for the binuclear complexes in "over-exchanged" Fe/ZSM5 in air at room temperature, based on the structures derived by Battiston and co-workers.[9] It shows the binuclear complexes (cylinders and balls) within the ZSM5 zeolite framework (thin lines), looking parallel to the 10-membered pores. The Fe atoms are bound to two O atoms of the zeolite framework neighboring an Al atom. In addition, they are connected via two hydroxo bridges to each other. Further bonding exists to a hydroxide group and to a water molecule. This yields two sixfold-coordinated sites. Figure 9a and b have been created with Cerius^2, using an optimization of the binuclear complexes with universal force field (UFF) parameters.[30] The zeolite lattice has been fixed and only the nonframework O, H, and Fe atoms were optimized. The two Al positions were chosen at a distance similar to the average Al−Al distance within ZSM5 for a Si/Al ratio of 17. Both Fe atoms in the structure are octahedrally surrounded, where the bottom Fe atom has a significantly distorted octahedron. The Fe−Fe distance is 3.05 Å in this structure, in agreement with the structure as derived from in-situ extended X-ray absorption fine structure (EXAFS) analysis.[9] For many Al−Al distances that allowed the formation of binuclear centers, the iron distances were constantly similar to this value.

Treatment in helium at room temperature reduces the valence state of Fe from 2.94 to 2.65 for the irradiated portion of the sample and to 2.49 for the nonirradiated portion. First, this implies that the X-rays affect the reduction significantly, a fact that must be kept in mind while performing (soft) X-ray experiments on sensitive materials. The average valence of ∼2.5 implies that, of the binuclear centers, on average, one Fe is reduced to Fe^{II}, and the other remains Fe^{III}. It could also indicate

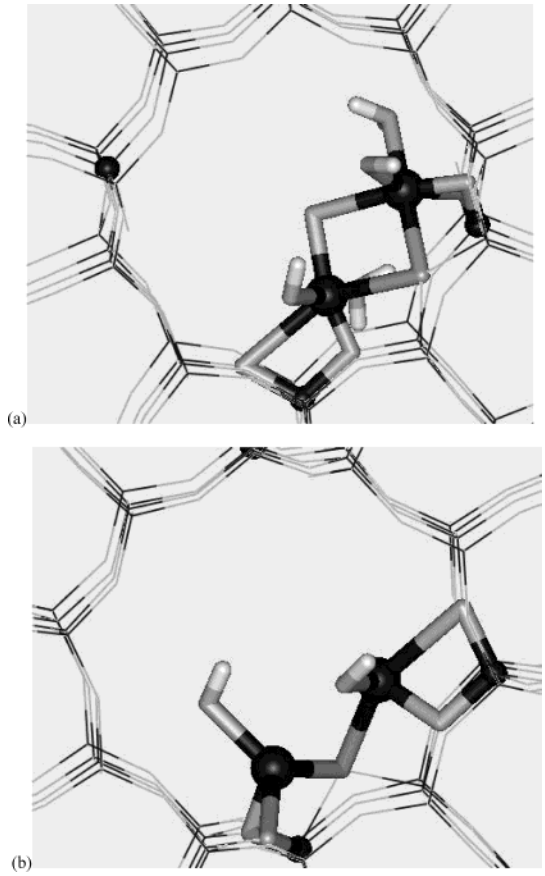

Figure 9. Models of possible structures for Fe/ZSM5 (a) at room temperature in air and (b) in helium at 350 °C. The binuclear center is highlighted within the ZSM5 zeolite framework (thin lines). Fe (big) and Al (small) atoms are indicated as black balls, O is indicated in gray (as gray lines in the framework and gray sticks in the binuclear center), H is represented as white sticks, and Si is represented as black lines.

that some of the binuclear complexes are more reactive than others (for example, because of the depth at which they are located within the channels or due to the anchoring site, i.e., the position of the Al binding atoms within the zeolite). Spectral shape analysis showed that the Fe^{II} site is (distorted) tetrahedral, which suggests the presence of binuclear centers that consist of a combination of octahedral Fe^{III} with tetrahedral Fe^{II}. The change from six to four neighbors implies that the Fe^{III} sites will have to lose water molecules. The analysis of the hard X-ray data in refs 8 and 9 suggested that, at lower temperatures, the number of neighbors is reduced faster than the change of the iron valance. This observation is further confirmed by the fact that the water loss is highest at ~60 °C. It can be concluded that a large amount of loosely bound water escapes from the zeolite at temperatures <100 °C and some of this water originates from the binuclear iron sites.

Heating in helium to 350 °C leads to a further reduction of Fe to an average valence of 2.16. This number is lower than the average valence of 2.4 that has been determined from hard X-ray absorption near-edge structure (XANES) analysis. This difference is probably due to the difference in probing depth (5 nm for the soft X-ray L-edges versus several micrometers for the hard X-ray K-edge. An average valence of very close to 2.0 implies that most of the iron is present in (binuclear) sites that consist of (two) tetrahedral Fe^{II} sites (in other words, the removal of two O neighbors from each Fe atom). Figure 9b shows a possible structure of the two tetrahedral sites. Starting with Figure 9a, the two bridging hydroxide groups lose water, where the bridging between the Fe atoms is modified to a free O atom and a framework O atom. In addition, the two water molecules are lost, followed by the loss of the bridging free O atom. This creates two Fe tetrahedral sites bridged only by a framework O atom. Note that, in the force field calculation also, this bridging framework O atom was optimized, as can be observed in Figure 9b. The Fe−Fe distance of this cluster is 3.00 Å, which confirms the trend that was determined from EXAFS.[9] The loss of oxygen and water is confirmed by the gas-phase oxygen signal. This observation implies that Fe^{II} sites are spatially close together, because they share a framework O atom. As we show in an upcoming publication, a reoxidation can readily restore the bridging O atom between these close Fe^{II} sites. Reoxidation in O_2 creates two octahedral Fe^{III} sites within a matter of minutes.

5. Conclusions

Charge-transfer multiplet calculations provide a detailed theoretical understanding of the $L_{2,3}$ spectra of iron in Fe/ZSM5. The oxidized form of Fe/ZSM5 has iron in an octahedral surrounding, with a total crystal-field splitting of ~1.0 eV, which is considerably less than that of bulk Fe_2O_3. This indicates much weaker Fe−O bonding. The reduced form of Fe/ZSM5 has a tetrahedral surrounding of oxygen.

The Fe^{II} and Fe^{III} L_3 X-ray absorption spectra allow for accurate determination of the valence under various conditions. The Fe species in Fe/ZSM5 undergo autoreduction to a valence of 2.68 in helium at room temperature. During heating to 350 °C, the valence is further reduced to 2.16. The introduction of oxygen causes fast reoxidation of the system to almost-pure Fe^{III}.

We have shown that in-situ soft X-ray absorption provides an additional tool to determine the oxidation/reduction behavior of Fe/ZSM5. It yields new information on the geometry and valence of the Fe sites and it yields an accurate method to determine the average iron valence during oxidation/reduction cycles.

Acknowledgment. The authors thank the BESSY staff for their continual support during the XAS measurements at the synchrotron in Berlin. The research of W.M.H. is supported by a grant from Netherlands Scientific Organization−Chemical-Sciences (NWO−CW), and the research of F.M.F.dG is supported by The Netherlands Research School Combination on Catalysis (NRSCC) and the Science Renewal Fund of NWO−CW.

References and Notes

(1) Knop-Gericke, A.; Hävecker, M.; Neisius, T.; Schedel-Niedrig, T. *Nucl. Instrum. Methods Phys. Res., Sect. A* **1998**, *406*, (2), 311−322.

(2) Hävecker, M.; Knop-Gericke, A.; Schedel-Niedrig, T. *Appl. Surf. Sci.* **1999**, *142*, 438−442.

(3) Knop-Gericke, A.; Hävecker, M.; Schedel-Niedrig, T.; Schlögl, R. *Top. Catal.* **2000**, *10*, 187−198.

(4) Panov, G. I.; Uriarte, A. K.; Rodkin, M. A.; Sobolev, V. I. *Catal. Today* **1998**, *41*, 365−385.

(5) Ribera, A.; Arends, I.; De Vries, S.; Perez-Ramirez, J.; Sheldon, R. A. *J. Catal.* **2000**, *195*, 287−297.

(6) Chen, H. Y.; Voskoboinikov, T.; Sachtler, W. M. H. *J. Catal.* **1998**, *180*, 171−183.

(7) Wang, X.; Chen, H. Y.; Sachtler, W. M. H. *J. Catal.* **2001**, *197*, 281−291.

(8) Battiston, A. A.; Bitter, J. H.; de Groot, F. M. F.; Overweg, A. R.; Stephan, O.; van Bokhoven, J. A.; Kooyman, P. J.; van der Spek, C.; Vankó, G.; Koningsberger, D. C. *J. Catal.* **2003**, *213*, 251.

(9) Battiston, A. A.; Bitter, J. H.; de Groot, F. M. F.; Heijboer, W. M.; Koningsberger, D. C. *J. Catal.* **2003**, *215*, 279.

(10) Garten, R. L.; Delglass, W. N.; Boudart, M. *J. Catal.* **1970**, *18*, 90−107.
(11) Lobree, L. J.; Hwang, I. C.; Reimer, J. A.; Bell, A. T. *J. Catal.* **1999**, *186*, 242−253.
(12) Joyner, R.; Stockenhuber, M. *J. Phys. Chem. B* **1999**, *103*, 5963−5976.
(13) Pérez-Ramírez, J.; Mul, G.; Kapteijn, F.; Moulijn, J. A.; Overweg, A. R.; Doménech, A.; Ribera, A.; Arends, I. W. C. E. *J. Catal.* **2002**, *207*, 113−126.
(14) Marturano, P.; Drozdova, L.; Pirngruber, G. D.; Kogelbauer, A.; Prins, R. *Phys. Chem. Chem. Phys.* **2001**, *3*, 5585−5595.
(15) Nováková, J.; Kubelková, L.; Wichterlová, B.; Juška, T.; Dolejšek, Z. *Zeolites* **1982**, *2*, 17−22.
(16) Jacobs, P. A. *Stud. Surf. Sci. Catal.* **1986**, *29*, 357−414.
(17) Chen, H. Y.; Sachtler, W. M. H. *Catal. Today* **1998**, *42*, 73−83.
(18) Battiston, A. A.; Bitter, J. H.; Koningsberger, D. C. *Catal. Lett.* **2000**, *66*, 75−79.
(19) Abbate, M.; Goedkoop, J. B.; De Groot, F. M. F.; Grioni, M.; Fuggle, J. C.; Hofmann, S.; Petersen, H.; Sacchi, M. *Surf. Interface Anal.* **1992**, *18*, 65−69.
(20) Outka, D. A.; Madix, R. J.; Stöhr, J. *Surf. Sci.* **1985**, *164*, 235.
(21) Van Aken, P. A.; Liebscher, B. *Phys. Chem. Miner.* **2002**, *29*, 188−200.
(22) Crocombette, J. P.; Pollak, M.; Jollet, F.; Thromat, N.; Gautier-Soyer, M. *Phys. Rev. B* **1995**, *52*, 3143−3150.
(23) Kuiper, P.; Searle, B. G.; Rudolf, P.; Tjeng, L. H.; Chen, C. T. *Phys. Rev. Lett.* **1993**, *70*, 1549−1552.
(24) Colliex, C.; Manoubi, T.; Ortiz, C. *Phys. Rev. B* **1991**, *44*, 11402−11411.
(25) de Groot, F. M. F.; Fuggle, J. C.; Thole, B. T.; Sawatzky, G. A. *Phys. Rev. B* **1990**, *41*, 928.
(26) de Groot, F. M. F.; Fuggle, J. C.; Thole, B. T.; Sawatzky, G. A. *Phys. Rev. B* **1990**, *42*, 5459.
(27) de Groot, F. M. F. *J. Electron. Spectrosc. Relat. Phenom.* **1994**, *67*, 529−622.
(28) de Groot, F. *Chem. Rev.* **2001**, *101*, 1779−1808.
(29) Hitchcock, A. P.; Stöhr, J. *J. Chem. Phys.* **1987**, *87*, 3253−3255.
(30) Cerius^2 is a modeling and simulation software package, created by Molecular Simulations, Inc. (MSI), which is now Accelrys. See http://www.accelrys.com/cerius2/.